Stony Brook University

Characterization of a genetic interaction between the Srs2 helicase and phosphorylated Zip1 during budding yeast meiosis

A Thesis Presented

by

Dimitri F. Joseph

to

The Graduate School

in Partial Fulfillment of the

Requirements

for the Degree of

Master of Science

in

Biochemistry and Cell Biology

Stony Brook University

May 2017

Stony Brook University

The Graduate School

Dimitri Joseph

We, the thesis committee for the above candidate for the

Master of Science degree, hereby recommend

acceptance of this thesis.

Nancy M. Hollingsworth – Thesis Advisor
Professor, Department of Biochemistry and Cell Biology

Ed Luk – Second Reader
Professor, Department of Biochemistry and Cell Biology

This thesis is accepted by the Graduate School

Charles Taber
Dean of the Graduate School

Abstract of the Thesis

Characterization of a genetic interaction between the Srs2 helicase and phosphorylated Zip1 during budding yeast meiosis

by

Dimitri F. Joseph

Master of Science

in

The Biochemistry and Cell Biology Master of Science Program

Stony Brook University

2017

Homologous Recombination (HR) is an essential mechanism for double strand break (DSB) repair that generates crossovers (COs). In meiosis, HR is required for proper chromosome segregation at the first meiotic divison. The Sgs1 helicase promotes the formation of non-crossovers (NCOs) through a process called synthesis-dependent strand annealing. A set of meiosis specific genes called the ZMM genes, protects strand invasion intermediates from Sgs1, resulting in the formation of a specific class of COs that are distributed throughout the genome. The transverse filament protein, Zip1 is encoded by one of the ZMM genes, and phosphorylation of Zip1 on four adjacent serines in its C terminus are required for the ZMM pathway of recombination. Previous work has shown the absence of SGS1 combined with a nonphosphorylatable version of *ZIP1*, *zip1-4A*, triggers the meiotic recombination checkpoint, resulting in meiotic prophase arrest. Srs2 is a less well studied helicase in meiosis, which like Sgs1, exhibits an anti-recombinase function during DSB repair in vegetative cells. The

goal of my thesis was to see whether depletion of *SRS2* has a similar genetic interaction *in zip1-4A*, which would suggest a role for *SRS2* during meiosis similar to *SGS1*.

Table of Contents

List of Figures and Tables

List of Abbreviations

Ade: adenine

AE: axial element

ATG: sequence of the start codon of an open reading frame

BLM: Bloom's helicase

bp: base pairs

C: Celsius

CO: crossover

DAPI: 4',6-diamidino-2-phenylindole

dHJ: double Holliday junctions

DNA: deoxyribonucleic acid

dNTP: deoxyribonucleotide triphosphates

DSB: double strand break

EDTA: ethylenediaminetetraacetic acid

G418: geneticin

GAD: Gal4 activating domain

HA: hemagluttinin

HR: homologous recombination

HygB: hygromycin B

Kb: kilobase

KoAc: potassium acetate

LiAc: lithium acetate

M: mole

MI: meiosis I

MII: meiosis II

mL: milliliter

NaOAc: sodium acetate

NAT: nourseothricin

NEB: New England Biolabs

nm: nanometers

PBS: phosphate buffered saline

PEG: poly ethylene glycol

OD: optical density

PCR: polymerase chain reaction

RPM: revolutions per minute

SAM: s-adenosyl methionine

SB: sample buffer

SC: synaptonemal complex

SIM: Sumo-interacting motif

SUMO: small ubiquitin-like modifier

SDS: sodium dodecyl sulfate

SDSA: synthesis dependent strand annealing

Spo: sporulation

ssDNA: single-stranded DNA

TBE: Tris Borate EDTA

TE: Tris EDTA

UV: ultraviolet

V: volts

X-gal: 5-bromo-4-chloro-3-indolyl-β-D-galactopyranoside

YPA: Yeast Peptone Acetate

YPD: Yeast Peptone Dextrose

Acknowledgements

I would like to thank Dr. Nancy M. Hollingsworth for giving me the opportunity to be a member in her lab. Under Dr.Hollingsworth's guidance, I have learned the necessary qualities to continue and achieve my scientific aspirations. I am grateful for being able to witness a world of mastery in science and research. Complementary to Dr. Hollingsworth, I would like to thank the Hollingsworth lab members past and present: Matthew Murray, Sana Hussain, Cameron Burnett, Xiangyu Chen, Bob Gaglione, Chris Pimental, Evelyn Prugar, and Lihong Wan for the inspiring conversations and for teaching me the techniques needed to complete this project. I'd like to especially thank Cameron Burnett and Xiangyu Chen for their patience and assistance in guiding me through obstacles that came along in this project. Lastly, I would like to thank Dr. Neta Dean for allowing me to use her microscope and Dr. Ed Luk for being my supplementary reader.

Introduction

Meiosis is a tightly choreographed cell division where a diploid parent divides to form four haploid daughter cells. In humans, meiosis produces gametes that are used in sexual reproduction. To achieve this goal, one round of DNA replication is followed by two rounds of chromosomal division. The first division segregates homologous chromosomes, while the second division segregates sister chromatids. For meiosis to proceed appropriately, programmed double strand breaks (DSB) are made by the highly conserved Spo11 endonuclease to initiate a repair mechanism that utilizes interhomolog recombination (Keeney, 2008). Repair using homologous chromosomes results in crossovers (COs) that are necessary for proper chromosome segregation at the first meiotic division. Errors in recombination may lead to aneuploid cells. In humans, aneuploid gametes may generate inviable fetuses or individuals with birth defects such as Trisomy 21 or Down syndrome.

Recombination begins in Prophase I, when Spo11 creates double strand breaks on one of the four sister chromatids in localized areas of the genome called “hotspots” (Keeney, 2008; Keeney et al., 1997) (Figure 1). The 5’ ends of the breaks are resected, leaving single stranded 3’ ends. These 3’ end are bound by the mitotic recombinase, Rad51, as well as the meiosis-specific recombinase, Dmc1, to form nucleoprotein filaments that perform template homology searches to repair the breaks (Brown et al., 2015; Shinohara et al., 1997). DSBs promote activation of the meiosis specific kinase, Mek1 (Niu et al., 2005). The presence of Mek1 activity in conjunction with the Dmc1 nucleoprotein circumvents repair from sister chromatids and strictly seeks homology on interhomologs (Niu et al., 2005). A nucleoprotein filament invades the non-sister

chromatid to form a displacement loop (D-loop). The 3' end is then used as a primer for DNA synthesis. As the invading strand elongates, the size of the D-loop is increased. After strand invasion, there are three different ways repair can occur. First, the Sgs1 helicase can unwind the extended invading strand from the template, which allows it to anneal to the 3' end on the other side of the DSB break to generate a non-crossover (NCO) in a pathway called synthesis dependent strand annealing (SDSA) (Allers and Lichten, 2001; McMahill et al., 2007). NCOs lack the required mechanical interaction between homologs to promote reductional division. The remaining two repair pathways generate COs through resolution of double Holliday junction (dHJ) intermediates that are formed when the displaced single strand of the D-loop anneals to the 3' end on the other side of the DSB. In the presence of a functionally diverse set of proteins called the "ZMMs", strand invasion intermediates are protected from disassembly by Sgs1, leading to the biased resolution of the resulting dHJs to make COs (Borner et al., 2004; Jessop et al., 2006). Double HJs formed in the absence of ZMM proteins are resolved by structure-specific nucleases such as Mus81-Mms4 in an unbiased fashion generating both COs and NCOs (Jessop and Lichten, 2008).

The *ZMM* genes encode proteins (Zip1, Zip2, Zip3, Zip4, Mer3, Msh4 Msh5 and Spo16) that promote the biased resolution of dHJs to produce COs as well as formation of the synaptonemal complex (SC) between homologous chromosomes (Lynn et al., 2007). The SC is a tripartite structure that regulates how DSBs will be repaired. Maternal and paternal sister chromatids condense and project from independent axial cores to form congruent structures called axial elements (AEs) (Figure 2). In the budding yeast, *Saccharomyces cerevisiae*, AEs are comprised in part by the meiosis

specific proteins, Red1, Hop1 and Rec8 (Klein et al., 1999; Smith and Roeder, 1997). AEs are brought together by recombination and then “glued” together by the insertion of the transverse filament protein Zip1 (Sym et al., 1993). The Zip1 protein contains amino and carboxy terminal globular domains flanking coiled-coiled regions that allow oligomerization between Zip1 molecules (Sym et al., 1993; Tung and Roeder, 1998). In frame deletion of a 25 amino acid region within the Zip1 C terminus prevents synapsis and significantly reduces spore viability (Tung and Roeder, 1998). Cdc7-Dbf4 phosphorylation of four adjacent serines in this region is required for the ZMM pathway of CO formation and synapsis (Chen et al., 2015). The *zip1-4D* allele substitutes the four serines with phosphomimetic, negatively charged aspartic acid residues. This mutant is phenotypically similar to *ZIP1* (Chen et al., 2015). In contrast, the *zip1-4A* mutant cannot be phosphorylated at these serines. Instead of polymerizing along the lengths of the chromosomes to form SCs, the Zip1-4A protein forms foci. The failure to synapse prevents the down-regulation of Spo11 activity, resulting in increased numbers of DSBs (Chen et al., 2015; Thacker et al., 2014). Unrepaired DSBs trigger the meiotic recombination checkpoint, which prevents the onset of Meiosis I (Lydall et al., 1996; Roeder and Bailis, 2000). The delay in DSB repair therefore results in a delay in meiotic progression, although the *zip1-4A* mutant is eventually able to sporulate. Spore viability is higher in *zip1-4A* than in a *zip1*Δ because the increased number of DSBs provides additional opportunities for CO formation by Mus81-Mms4 (Chen et al., 2015).

Sgs1 is a 3’ to 5’ helicase that antagonizes the ZMM pathway to prevent the presence of aberrant recombination intermediates (Muyt et al., 2012; Oh et al., 2007). It is orthologous to the mammalian Bloom’s (BLM) helicase which, when mutated, results

in chromosomal instability that promotes premature aging and cancer (Watt et al., 1996). Sgs1 directs recombination intermediates to be repaired using the synthesis dependent strand annealing (SDSA) pathway. Zip1 and Sgs1 antagonize each other to resolve DSBs as either COs or NCOs, respectively (Hussain, 2013; Jessop et al., 2006) This idea is based on the observation that deleting *SGS1* partially suppresses the CO defect of *zmm* mutants, including *zip1*Δ (Jessop et al., 2006; Oh et al., 2007). The conclusion is that in *zmm* mutants, most DSB repair is directed down the SDSA pathway via Sgs1. When *sgs1* is also deleted, DSBs are processed by the unbiased resolution of dHJs by the SSNs (Jessop and Lichten, 2008).

Combining a meiotic depletion allele of *SGS1*, *sgs1-md,* with *zip1-4A* resulted in a gain of function phenotype in which *sgs1-md zip1-4A* cells arrested in meiotic prophase (while *sgs1-md zip1*Δ cells did not) (Chen et al., 2015). This observation, coupled with the observations that (1) Zip1-4A protein exhibits discrete foci, (2) Zip1 is recruited to DSBs during meiosis (Shinohara et al., 2015) and (3) the C-terminus of Zip1 interacts with a fragment of Sgs1 in the two-hybrid system (Hussain, 2013), led to the model that Zip1 is first recruited to DSBs after which there are two possible fates: (1) Zip1 is phosphorylated by Cdc7-Dbf4 and the break is repaired by the ZMM pathway allowing for synapsis or (2) Sgs1 removes unphosphorylated Zip1 from the break which can then try again or be repaired by either SDSA or the SSN pathways (Chen et al., 2015). In the *sgs1-md zip1-4A* mutant, DSBs bound by Zip1 are not repaired by the ZMM pathway nor can the protein be removed by Sgs1, and the persisting broken ends trigger a meiotic recombination checkpoint arrest.

Srs2 is a 3’ to 5’ helicase that helps maintain genomic integrity by reducing the prevalence of COs from DSBs in mitotic cells (Ira et al., 2003). In vegetative growth, homologous recombination is critical to repair DNA DSBs and to resume DNA replication at aberrant replication forks (Esta et al., 2013). Srs2 can remove the Rad51 recombinase from single-stranded DNA thus preventing strand invasion at untimely points in DNA replication (Antony et al., 2009; Krejci et al., 2003) . Like *sgs1*, in *srs2Δ* cells, two phenotypes have been noted: (1) there is an increase in COs which may lead to genomic instability (2) the cells are more susceptible to DNA damage that result from the presence of detrimental recombination intermediates that persist (Esta et al., 2013). In meiotic cells overexpression of *SRS2* dismantles Rad51 from 3’ ssDNA preparing to perform a homology search (Krejci et al., 2003). *SRS2* overexpression has an adverse effect on the ability to repair DSBs (Sasanuma et al., 2013). Recently a two hybrid screen using the *ZIP1* C terminus containing the four aspartic amino acid substitutions as bait identified two plasmids containing overlapping inserts of *SRS2* (Murray, 2015). The parallels between *SRS2* and *SGS1* (both are 3’ to 5’ helicases involved in mitotic recombination and interact with the C-terminus of Zip1) led to the following questions addressed in my thesis: (1) Are the requirements for interaction with Zip1 the same between the two helicases and (2) Is there a synthetic interaction between *srs2* and *zip1-4A* with regard to meiotic progression, similar to what is observed for *sgs1* and *zip1-4A*?

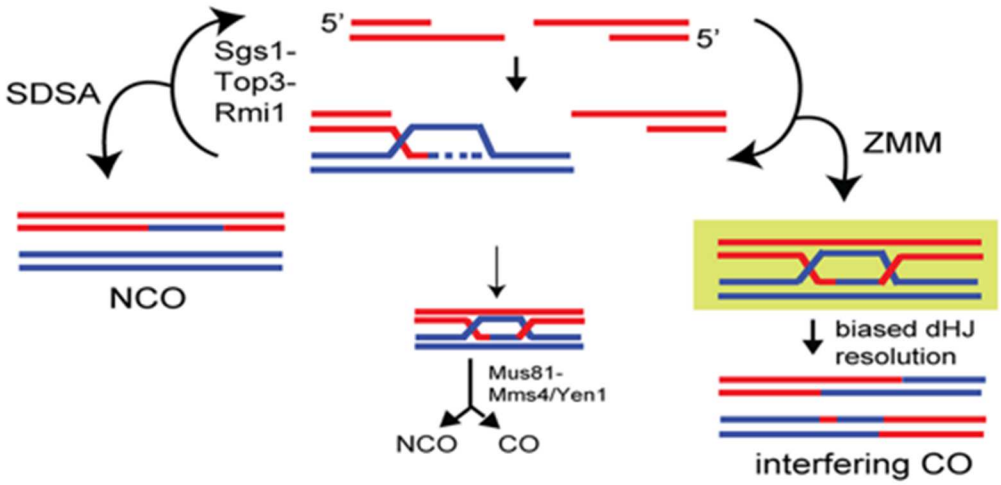

Figure 1. The different steps in meiotic recombination. In the first step of meiotic recombination DSBs are formed and the 5' ends are resected. (Only one of the four chromatids is shown). Next, a 3' single strand invades the duplex DNA from the homolog to form a displacement or D-loop. (Only a pair of non-sister chromatids is shown). The invading strand then primes DNA synthesis. The DSBs may then be repaired in one of three pathways. (1) Synthesis-dependent strand annealing (SDSA): displacement of the extended invading strand by Sgs1 results in annealing of the end to the other side of the break to create NCOs that contain matching parental flanking regions. (2) Strand invasion intermediates are stabilized by the ZMM pathway to create double Holliday junction intermediates that are biased to be resolved as COs that have flanking regions from different parental homologs. These COs are distributed throughout the genome by genetic interference. (3) Double Holliday junction intermediates that arise in the absence of the ZMM proteins are resolved by structure selective endonucleases such as Mus81-Mms4 or Yen1 which resolve the junctions in an unbiased fashion to produce both CO and NCOs. Figure has been adapted from (Muyt et al., 2012).

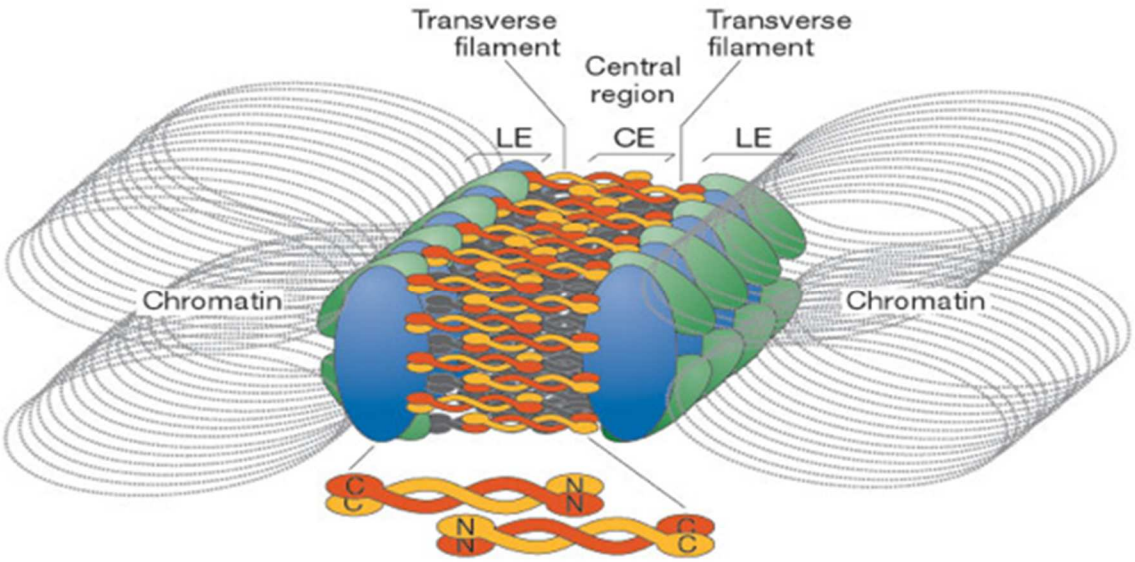

Figure 2. A model of the synaptonemal complex (SC). Axial elements (AEs) are formed by condensation of sister chromatids along protein cores which in yeast contains the meiosis-specific proteins Red1, Rec8 and Hop1. Interhomolog recombination mediated by the ZMM pathway brings homologous AEs together which are then held together by the transverse filament protein Zip1, to form the SC. In the context of the SC, AEs are referred to as lateral elements. Zip1 is a coiled-coiled protein flanked by two globular domains. The C-terminal domain interacts with the LE, and the N-terminal domain of two Zip1 filaments overlap in the middle of the central region to form the central element. Figure is taken from (Page and Hawley, 2004).

METHODS

Yeast strains and media.

The genotypes of the strains used in this study are provided in Table 1.

YPD liquid medium**:** 2% bactopeptone, 1% yeast extract, 0.1% glucose

YPA liquid medium: 1% yeast extract, 2% bactopeptone, 2% potassium acetate

YPglycerol solid medium: 2% agar, 2% peptone, 1% yeast extract

YPD Com solid medium: 2% bactoagar, 2% bactopeptone, 1% yeast extract, 2% glucose, 0.2% complete powder

Sporulation (Spo) liquid medium: 2% potassium acetate

Spo solid medium**:** 2% bactoagar, 0.05% dextrose, 0.1% yeast extract, 2% potassium acetate + 0.2% complete powder

SD solid medium: 2% bactoagar, 0.7% yeast nitrogen base without amino acids, 2% glucose

SD solid medium lacking various amino acids and/or bases was made by adding 4 g/L dropout powders lacking the appropriate nutrient. The composition of the dropout powder is given in (Lo and Hollingsworth, 2011).

Antibiotic-containing YPDcom plates were generated using the following final drug concentrations: 0.02% Geneticin (G418); 0.01% Nourseothricin (NAT); 0.03% Hygromycin B (HygB).

Yeast two-hybrid β-galactosidase filter assay

L40 cells co-transformed with *lexA* and *GAD* fusion plasmids (marked with *TRP1* and *LEU2*, respectively) were patched onto SD-Trp-Leu plates and grown at 30°C

overnight. The patches were then replica plated to a second SD-Trp-Leu plate to make a master copy and an SD-Trp-Leu plate layered with a Whatman 1450-082 filter. The cells were grown overnight at 30°C. For the β-galactosidase enzyme assay, 2 mL of 1x Z buffer (60 mM Na_2HPO_4, 40 mM $NaH_2PO_4 \cdot H_2O$, 10 mM KCl, 1mM $MgSO_4 \cdot 7H_2O$, 4 mM 2-mercaptoethanol) + 20 μL 3% 5-bromo-4-chloro-3-indolyl-β-D-galactopyranoside (X-gal), dissolved in dimethyl formamide, was placed into an empty petri dish. A Whatman 1003-082 filter was placed on top of the solution to evenly absorb the liquid. The filter containing the cells was immersed in liquid nitrogen for approximately 10 seconds to lyse the cells. This filter was then placed (cell side up) on the filter in the petri dish and incubated at 30°C. The patches on the filters were regularly surveyed for up to three hours for the appearance of a blue color indicative of X-gal cleavage by β-galactosidase.

Polyermase chain reaction

Two types of polymerase chain reactions (PCR) were performed. The sequences of all of the primers used for this thesis are given in Table 2. The first type used Vent polymerase and the plasmid, pRK69, to generate a 2.7 kb fragment containing *kanMX6* and P_{CLB2}-*3HA* flanked by homology around the *SRS2* promoter. Each reaction contained 2.5 μL of 20 ng/μL of pRK69 template,10.0 μL 10 X Thermo Pol Buffer, 10 μL 2 mM deoxyribonucleotides (dNTPs), 5 μL of 10.0 μM of SRS2-CLB2-F4 and SRS2-CLB2-R3, 66.5 μL water, and 1 μL of Vent polymerase. Eight 100 μL reactions were aliquoted into 0.2 mL PCR tubes and placed in a thermocycler. After the initial one minute denaturing step at 95°C, the reactions cycled 35 times through a 95°C

denaturing step for thirty seconds, a 54°C annealing step for one minute and a 72°C extension step for two minutes and thirty seconds. After the cycles were complete, the reactions were held at 20°C or placed at -20°C. The success of the reactions was determined by combining 10 μL of each reaction with 2 μL of 6 X DNA sample buffer (SB)[10 mM Tris-HCl, pH 7.6, 0.03% bromophenol blue, 0.03% xylene cyanol FF, 60% glycerol, 60 mM Ethylenediaminetetraacetic Acid (EDTA)] and running the samples on a 0.8% 0.5 X Tris-Borate-EDTA (TBE) agarose gel for approximately one hour at 100 volts (V). The running buffer contained 10 μL of 10 mg/mL ethidium bromide to stain the DNA. The DNA was then visualized using a short wave ultraviolet (UV) light transilluminator.

To precipitate the DNA, the eight PCR reactions were divided into two separate microfuge tubes of 400 μL each. 40 μL of 3 M sodium acetate (NaOAc), pH 5.2, and 440 μL of isopropanol were added to each tube. The samples were vortexed and left at room temperature for 5 minutes to allow precipitation. The DNA was pelleted by microcentrifugation at 14,000 revolutions per minute (rpm) in an Eppendorf Centrifuge 5418 R for 10 minutes. The pellets were then rinsed with 1 mL of cold 70% ethanol. The tubes were placed upside down on a paper towel for 10 minutes to air dry the DNA. Each pellet was resuspended in 40 μL of 1 X TE, pH 8 (10 mM Tris-HCL, pH 8.0, 1mM EDTA, pH 8.0) and pooled with the DNA from the other reactions. One μL of DNA + 9 μL of 1x TE + 6X DNA SB was run on a 0.8% TBE agarose gel to confirm the appropriate fragment of concentrated DNA. The DNA was stored at -20°C.

A second type of PCR reaction was used to detect the presence of the P_{CLB2}-*SRS2* allele in the chromosome. These reactions used crude DNA isolated from

different transformants as the templates. Crude DNA was generated using a pipette tip to transfer freshly grown transformants into microfuge tubes that carried 30 μL of 0.2% sodium dodecyl sulfate (SDS). The tubes were vortexed for 15 seconds, heated at 95°C for 4 minutes and the cells pelleted in a microcentrifuge by spinning for 1 minute at 14,000 rpm. 25 μL of the supernatant containing the crude DNA was moved to a clean microfuge tube. Three microliters of crude DNA was added to a 50 μL PCR reaction containing 5 μL 10 X Choice Taq buffer, 2 μL 25% Triton X-100, 5 μL 2 mM dNTPs, 29.5 μL water, 0.5 μL Taq polymerase and 2.5 μL of 10 μM of KAN-IN and SRS2-IN primers. After a 1 minute denaturing step at 95°C, the PCR reactions cycled 35 times through a 95°C denaturing step for thirty seconds, a 54°C annealing step for one minute and a 72°C extension step for one minute and thirty seconds. After all the cycles were finished, the reactions were held at 20°C or moved to -20°C. The predicted band of 1.6 kb was determined using a 0.8% TBE agarose gel.

Yeast Transformation

The 2.7 kb *kanMX6-pCLB2-3HA* fragment with flanking *SRS2* homology and the p382, p382-4A, pRS304 integrating plasmids (digested with BsgI) were transformed into SK1 strains while the 2μ *lexA* and *Gal4 activation domain* (*GAD*) plasmids were co-transformed into the L40 strain. Sterile toothpicks were used to inoculate cells into 15 mL test tubes containing 2 mL of YPD [+ 0.02% adenine (ade) for L40]. Cells were vortexed and grown overnight on a roller at 30°C. Overnight cultures were diluted into 100 mL of YPD (+0.02% adenine for L40) in 500 mL flasks and shaken at 250 rpm at

30°C for 5 hours. The cells were transferred to 250 mL bottles and pelleted at 5000 rpm for 10 minutes in a GSA rotor using a Sorvall centrifuge. The pellets were resuspended in 10 mL of water, transferred to 15 mL test tubes and spun for 5 min in a tabletop centrifuge. Sonicated salmon sperm DNA was denatured to make 10 mg/mL of single-stranded DNA (ssDNA) by incubation at 95°C for five minutes and then put on ice. Cell pellets were resuspended in 0.5 mL of LiAc-TE, pH7.5 (0.1 M LiAc, pH7.5, 1 mM EDTA pH7.4, 10 mM Tris-HCl pH 7.5). 100 μl cells were aliquoted into each microfuge tube along with 10 μL of 10 mg/mL ssDNA, 0.7 mL 100 mM LiAc-40% polyethylene glycol (PEG), (0.1M LiOAc, pH7.5, 1mM EDTA pH7.4, 10mM Tris-HCl pH 8, 0.4 M PEG and 10 μL *kanMX6-pCLB2-3HA*, 5 μL of 100 ng/μL of the digested plasmids, or 3 μL of 50 ng/μL of the 2μ plasmids for the L40 co-transformation. After mixing, each reaction was incubated at 30°C for 30 minutes and then heat shocked at 42°C for 15 minutes. The cells were pelleted in a picofuge for 1 min and the supernatants were aspirated with sterile pipette tips. For the *kanMX6* transformation, the cells were resuspended in 500 μl of liquid YPD and transferred to a test tube that carried 2 mL of YPD. These cells were incubated in a roller at 30°C. After an hour, the cells were spun down in a tabletop centrifuge for 5 minutes. Each pellet was resuspended in 300 μL of water and spread onto two selective plates and the cells were grown at 30°C for three days.

Mating type tests

For mating type identification, cells under investigation were replica plated to a YPD plate, cross stamped with mating type testers and grown at 30°C overnight. To transfer the tester cells, the side of a sterile wooden popsicle stick was used to pick up

cells from a lawn of either *MAT***a** *lys1* or *MAT*α *lys1* which were then pressed onto the replica plated cells on the YPD plate. The cells were allowed to mate and grow at 30°C overnight and then were replica plated onto an SD plate. The tester strains cannot grow on SD because they are auxotrophic for lysine, while the sample strains are auxotrophic for uracil. Only when a sample strain mated with a tester of opposite mating type was a prototrophic diploid capable of growing on minimal medium generated. Therefore colonies that grow on the SD plate are of opposite mating type to the tester strain. Sample cells that are diploid are unable to mate with either tester strain.

Plasmid digestion with BsgI

TRP1-integrating plasmids p382, p382-4A and p382-4D, were digested with BsgI to target integration of the plasmids to the 3' end of the *trp1-5'*Δ allele. BsgI requires S-adenosyl methionine (SAM). A fresh stock of 10 X SAM was made by combining 2 μL 32 mM SAM, 8 μL 10 X New England Biolabs (NEB) Buffer 4, and 70 μL of water. Plasmid digests were performed in a total volume of 50 μL and contained 5 μL 10 x SAM buffer, 5 μL Cutsmart or NEB4 buffer, 2.5 μL of 5 units/μL BsgI, and 5 μg plasmid DNA. Water was added to make up the volume to 50 μL. The reaction mixtures were incubated at 37°C for 3 hours. The digests were confirmed by running 1μL of 100 ng/μL of DNA with 9 μL 10X TE and 2 μL of 6X DNA SB on a 0.8% TBE agarose gel.

Meiotic Time Courses

Fresh transformants were patched onto YP glycerol plates to test for petite mutants and the remaining cells were inoculated in 5 mL YPD in a 15 mL test tube and

grown overnight at 30°C in a roller. Petite cells have defective mitochondria and therefore grow at a slower rate in complete medium containing glucose. When the medium contains a non-fermentable carbon source such as potassium acetate (KOAc), which is used to induce meiosis, petite cells do not grow at all and fail to sporulate. Petite strains should therefore not be used for meiotic experiments. After 16 hours, 0.8 mL and 1.3 mL of the overnight cultures were diluted into two 500 mL flasks, respectively, containing 50 mL of yeast peptone acetate (YPA) liquid medium. The cultures were then shaken at 250 rpm on a shaker at 30°C for 15 hours. One mL of each culture was used to measure the optical density (OD) at wavelength 660 nm with a spectrophotometer. Cells with OD_{660} readings between 1.3 – 1.6 were transferred to a sterile 250 mL bottle and centrifuged down at 10,000 rpm on a GS3 rotor in a Sorvall centrifuge. The supernatants were removed and the pellets resuspended in 10 mL of water, transferred to 15 mL test tubes and pelleted again using a tabletop centrifuge. Each cell pellet was resuspended in a volume of 2% KoAc (called Spo medium) at a cell density of 3 X 10^7 cells/mL using the following formula:

$$\frac{\frac{\#\ \text{of cells/mL}}{2} \times 300\ \text{mL YPA}}{3 \times 10^7\ \text{cells/mL}} = \text{Volume of Spo Medium}$$

Cell density was determined using a table that converts OD_{660} values to a haploid cell concentration(Lo and Hollingsworth, 2011). Meiotic experiments use diploid cells that are larger than haploid cells. Dividing the haploid cell density obtained from the table in half adjusts for diploid cells which are bigger and thus produce a higher optical density reading than haploid cells. The same volume of each culture (equivalent to the one with the lowest amount of Spo medium) was transferred to 125 mL flasks. Samples were

taken for the 0 timepoint and the flasks were then placed in a 30°C shaker at 250 rpm. At 2 hour intervals, 0.5 mL culture was transferred into microfuge tubes that contain 50 μL 37% formaldehyde, vortexed and stored at 4°C. Meiotic progression was assayed by fluorescence microscopy (see below) while the percentage of sporulating cells was determined by counting the number of cells that formed asci using light microscopy. For each timepoint, 200 cells were counted.

Assaying meiotic progression

To stain cells with 4',6-diamidino-2-phenylindole (DAPI), 10 μL of 1X phosphate buffer solution (8% NaCl, 0.2% KCl, 1.44% Na_2HPO_4 0.24% KH_2PO_4) was added to wells in a Carlson Scientific, Inc. #101204 slide. 5μL of fixed cell samples from the meiotic time course were vortexed and added to each well with PBS. After 10 minutes, the liquid was aspirated and each well was washed three additional times with 10 μl PBS. After the final wash, 2 μL VectaShield with DAPI was added to each well. After sitting for 5 minutes, the cells were viewed in using a Axioskop 2 Plus fluorescence microscope at 40 X magnification. For each timepoint, the number of nuclei in 200 cells were counted. Mononucleates illustrate cells that have not completed meiosis, binucleates represent completion of Meiosis I, where tetranucleate cells indicate completion of Meiosis II.

Results

Srs2$^{1035\text{-}1074}$ interacts with the C-Terminus of Zip1 independently of negative charges at serines 815-818

The Zip1 C terminal globular domain is phosphorylated on serines 815-818 and this is required for the ZMM pathway of DSB repair and synapsis (Chen et al., 2015; Tung and Roeder, 1998). To identify proteins that interact with the Zip1 C-terminus, Matt Murray performed a yeast two hybrid screen using *lexA-Zip1C*-4D* as bait (Murray, 2015). The *lexA-ZIP1C*-4D* allele has the sequence for the bacterial DNA binding domain, l*exA*, fused to the C-terminus of Zip1 (amino acids 750-875). It encodes a protein with four aspartic acid substitutions in place of serine residues at positions 815 – 818. Previous work has shown that these negatively charged aspartic acids successfully mimic the negative charges conferred by phosphorylation *in vivo* (Chen et al., 2015). Two plasmids containing overlapping inserts of the *SRS2* gene, *GAD-SRS2*$^{1035\text{-}1174}$ and *GAD-SRS2*$^{879\text{-}1174}$ were isolated from this screen (Murray, 2015). What was not determined in these experiments was whether the negative charges on Zip1 promote the interaction with Srs2.

One way to detect protein-protein interactions using the two-hybrid system is to perform β-galctosidase assays. The L40 yeast strain contains the *lacZ* gene with multiple lexA binding sites in the promoter region (Criekinge and Beyaert, 1999). The lexA DNA binding domain localizes to the *lacZ* promoter, thereby tethering proteins of interest at this site (Chien et al., 1991). *GAD* plasmids contain the Gal4 activation domain which by itself does not localize to the *lacZ* promoter. Interaction between a GAD-protein fusion with a lexA-protein fusion brings the activation domain specifically to

the *lacZ* promoter, resulting in *lacZ* expression and the production of the enzyme β-galactosidase (Sternglanz, 1994). 5-bromo-4-chloro-3-indolyl-β-D-galactopyranoside (X-gal) is a β-galactosidase substrate. When X-gal is cleaved by β-galacotosidase, 5,5'-dibromo-4,4'-dichloro-indigo is formed and produces a blue color. The resulting blue color therefore indicates there is a protein-protein interaction between the lexA and GAD fusion proteins.

Two-hybrid assays with *GAD-SRS2*$^{1035-1174}$ and various *lexA-ZIP1C** mutants were conducted to test whether negative charges on the Zip1 C terminus influence its ability to interact with Srs2. *GAD-SRS2*$^{1035-1174}$ was co-transformed with plasmids carrying *lexA-ZIP1C*-WT*, *lexA-ZIP1C*-4A or lexA-ZIP1C*-4D.* The *lexA-ZIP1C*-4A* gene encodes alanine substitutions to prevent phosphorylation. *GAD-RED*$^{537-827}$ was used as a positive control which has previously been shown to interact with *lexA-ZIP1C*-WT* (Hussein, 2014) (Cheng et al, 2006) (Figure 3A). In addition, *GAD-REC8*$^{133-433}$ was previously identified to have an interaction with lexA-Zip1C* that is enhanced by negative charges at the 815-818 positions (Murray, 2015) (Figure 3A). *GAD-SRS2*$^{1035-1174}$ exhibited an interaction with all three lexA-*ZIP1C** alleles, indicating that the negative charges at amino acids 815-818 are not necessary for the Srs2 protein-protein interaction (Figure 3A).

The SUMO interaction motif in the Zip1 C terminus is not required for interaction with GAD-Srs2$^{1035-1174}$

The small ubiquitin-like modifier (SUMO) protein is a post-translational modification that promotes synaptonemal complex (SC) assembly (Karen Voelkel-

Meiman et al., 2013). Chains of SUMO proteins interact with the SUMO-interaction motif (SIM) in Zip1 and further assist the elongation of the SC (Cheng et al., 2006; Wang and Dasso, 2009). The function of this motif is abolished by substituting E862, D863 and Q864 for arginine (Cheng et al., 2006). The Zip1 C-terminal SIM is required for interaction with *GAD-RED1*$^{537-827}$ and *GAD-SGS1*$^{81-614}$ in the two-hybrid system (Hussain, 2013)(Figure 3B). Eight out of 17 transformants containing *lexA-ZIP1C*-3R* and *GAD-SRS2*$^{1035-1174}$ exhibited β-galactosidase activity (Figure 3B). The variability in β-galactosidase expression may be a consequence of a relatively low affinity between the lexA-Zip1C*-3R and GAD-Srs2$^{1035-1174}$ proteins. The genes were introduced into cells using 2μ plasmids that are present in a range from 50 - 100 copies/cell (Clark-Walker and Miklos, 1974). In some transformants, the plasmid copy number may be beneath the threshold needed to generate amounts of one or both proteins to generate a detectable amount of *lacZ* expression. The fact that some transformants exhibited β-galactosidase activity suggests that the Zip1 SIM is not required for interaction with Srs2. The ways that Sgs1 and Srs2 bind to the Zip1 C terminus are therefore not the same.

The Srs2$^{1035-1174}$ interaction with the Zip1 C terminus does not require amino acids 791-824

The Zip1 C terminal domain is an important region for localization of Zip1 to chromosomes and to mediate modifications such as sumoylation and phosphorylation that promote SC development (Chen et al., 2015; Cheng et al., 2006). An in-frame deletion of the codons specifying amino acids 791-824 in Zip1 results in a reduction in

spore viability and loss of synapsis (Tung and Roeder, 1998). This region is required for the *lexA-ZIP1C*-WT* interaction with *GAD-RED1*$^{537-827}$, but not *GAD-SGS1*$^{81-614}$ (Hussain, 2013) (Figure 3B) Yet, in my hands, both *GAD-RED1*$^{537-827}$ and *GAD-SGS1*$^{81-614}$ interaction with *lexA-ZIP1C*-WT* were diminished from deleting amino acids 791-824. For *GAD-SRS2*$^{1035-1174}$, 8 out of 17 transformants showed an interaction between *GAD-SRS2*$^{1035-1174}$ and *lexA-ZIP1C*-Δ791-824.* The intensity of the blue color from the galactosidase assay varied from dark blue to no color, likely due to variability in the 2μ plasmid copy number.

Placing the *SRS2* gene under the control of the *CLB2* promoter creates a meiotic depletion allele of *SRS2*

To generate a meiotic depletion allele of *SRS2*, the *SRS2* promoter was replaced in the chromosome with the promoter from *CLB2*. The *CLB2* promoter regulates the mitotic cell cycle and is expressed in vegetative cells only (Dahmann and Futcher, 1995). This promoter can therefore be used to deplete *SRS2* from meiotic cells, similar to what has been with SGS1(Jessop and Lichten, 2008). The SRS2-F4 and SRS2-R3 primers were used in a PCR reaction with the pRK69 plasmid to amplify a 2.7 kb *kanMX6-pCLB2-3HA* fragment with flanking homology to the *SRS2* promoter. The forward primer is located 100 base pairs (bp) upstream of the *SRS2* ATG start codon while the reverse primer starts 50 bp downstream of the ATG (Figure 4A). The resulting recombination event deletes 50 bp immediately upstream of the *SRS2* ATG and replaces it with the *CLB2* promoter (Figure 4B). In addition, integration of this fragment creates an in frame fusion of the 3 hemagglutinin (HA) epitope tag sequence to the 5'

end of the *SRS2* gene. The generation of the *kanMX6-pCLB2-3HA* fragment was confirmed on an agarose gel (Figure 5A). This fragment was then used to transform two SK1 strains: NHY1215 *trp1 zip1* and NHY1210 *trp1 zip1*. Transformants were selected by growth on G418^R, a drug to which *kanMX6* confers resistance (Hentges et al., 2005)

No transformants were observed for the NHY1210 trp1 zip1 strain, while 27 transformants were observed for the NHY1215 *trp1 zip1::natMX*- XC. These transformants were patched onto a YPD com plate, grown at 30°C overnight and then replica plated to YPD glycerol plates to eliminate transformants that were petite. Petite cells have defective mitochondria, causing the cells to depend on glycolysis for ATP production (Dunn et al., 2005). Glycolysis requires fermentable carbon sources such as dextrose. Using glycolysis as the sole source for ATP production results in slow growth on YPD com medium, resulting in smaller colony size (Dunn et al., 2005). In medium using non-fermentable carbon sources, glycolysis cannot be used so no ATP is produced. Therefore petite cells do not grow on glycerol or nor can they undergo meiosis in Spo medium which is composed of potassium acetate (KoAc). Any transformants that failed to grow on YPglycerol were discarded.

Three antibiotic resistance genes are used for making deletions/promoter fusions, *kanMX6*, *hphMX4* and *natMX6*. Each of these genes are amplified from various forms of the pFA6 plasmid, and they share regions of homology that flank the antibiotic resistance genes (Goldstein and McCusker, 1999). *hphMX4* and *natMX4* were previously integrated into the NHY1215 trp1 zip1 strain to delete *TRP1* and *ZIP1*, respectively. It was therefore possible that some G418^R transformants resulted from recombination between the *kanMX6-pCLB2-3HA* fragment in which the ends were

chewed back by exonucleases and the homology surrounding either *hphMX4* of *natMX4*. This type of recombination results in G418^R transformants that are sensitive to either HygB or NAT, respectively. The transformants were therefore also replica plated to YPDcom + HygB and YPDcom + NAT plates. Growth on each of these drug plates confirmed that the *kanMX6* marker had not simply replaced an existing drug-resistance marker. Seven out of 28 transformants retested as G418^R. Three of these seven patches were sensitive to either *HygB* or *nat* and were eliminated. Colony PCR was performed on the remaining four transformants using the SRS2-IN and KAN-IN primers to amplify a 1.6 kb fragment indicative of a P_{CLB2}-*SRS2* fusion gene (Figure 4C). Only one transformant showed the predicted fragment (Figure 5B). This transformant was named NHY1215 *trp1 zip1::nat XC srs2-md* and has the genotype: *MAT*α *leu2::hisG his4-LEU2-(NgoMIV + ori) ho::hisG ura3(*Δ*Sma-Pst) trp1-5'*Δ*::hphMX4 zip1*Δ*::natMX4 kanMX6::*P_{CLB2}*-3HA-SRS2*. This transformant was frozen at -80°C.

Because no transformants were obtained using the *MAT***a** *trp1 zip1* haploid, the *srs2-md* and *zip1*Δ*::natMX4* alleles from the *MAT*α haploid were introduced into a *MAT***a** strain by crossing NHY1215 trp1 zip1 XC srs2-md with NHY1210 trp1 on a YPDcom plate. The cells were grown at 30°C overnight, and then replica plated to an SD-his plate to select against the *MAT*α parent, which is auxotrophic for histidine. The remaining His$^+$ cells represent a mixture of *MAT***a** haploid and *MAT***a**/*MAT*α diploid cells that are prototrophic for histidine. The cells on the SD-his plate were replica plated to a Spo plate to induce sporulation and 51 tetrads from this cross, NH2393, were dissected by Lihong Wan. The spore viability from this diploid was 94%, indicating that neither *srs2-md* nor *zip1*Δ are haploid insufficient for spore viability. To identify *MAT***a** haploids

that carried the *srs2-md* and *zip1Δ::natMX4* alleles, as well as determine the genotype for other markers, spore colonies were screened for auxotrophy for uracil, tryptophan, leucine, histidine, as well as resistance to G418, NAT, and HygB.

*MAT**a*** haploids that were $G418^R$, and NAT^R contained *kanMX6*::*srs2-md* and *zip1Δ::natMX4*, respectively. NH2393 is homozygous for *trp1-5'Δ::hphMX4, LEU2 and ura3* and all of the spores were Trp^-, $HygB^R$, Leu^+ and Ura^- as expected. *HIS4* is heterozygous in NH2393 and the spore colony containing the desired genotype, NH2393-6-4, is prototrophic for histidine and therefore contains *HIS4*. NH2393-6-4 was picked as the *MAT**a** trp1-5'Δ::hphMX4 zip1Δ::natMX4 kanMX6::srs2-md* haploid to be used for diploid construction.

To make diploids that are heterozygous or homozygous for *srs2-md*, NH2393-6-4 was crossed with NHY1215 trp1 zip1 XC and NHY1215 trp1 zip1 XC srs2-md to generate NH2400 and NH2401, respectively. The crosses were replica plated to SD-his to select against MATα haploids. To isolate the diploids from the His^+ mating mixture, cells were streaked to generate single colonies that were then patched onto a YPDcom plate. The patches were replica plated to YPglycerol to eliminate petites and to YPCom where they were cross-stamped with the mating type testers for mating type tests. The patches that failed to mate with both the *MAT**a** lys1* and *MATα lys1* strains were indicative of diploids. One patch from each diploid was inoculated into 2 mL YPD, grown overnight and the diluted 1:1 with 50% glycerol and stored at -80°C.

Introduction of various *ZIP1* alleles into *srs2-md* heterozygous and homozygous diploids

The goal of my thesis was to determine whether there is a synthetic effect on meiotic progression when *srs2-md* is combined with the *zip1-4A* allele, similar to what was observed between the *sgs1-md* helicase mutant and *zip1-4A* (Chen et al., 2015). It was therefore necessary to generate *srs2-md* heterozygous and homozygous diploids containing *zip1*Δ, *ZIP1*, or *zip1-4A*. The integrating vector pRS304 (*TRP1*) and plasmids p382 (*TRP1 ZIP1*) and p382-4A (*TRP1 zip1-4A*) were digested with BsgI to target integration to the 3' end of the *trp1-5'*Δ allele in the *SRS2/srs2-md* and *srs2-md/srs2-md* diploids (NH2400 and NH2401, respectively). Plasmid integration introduces a single copy of each *ZIP1* allele, which is therefore hemizygous. The plasmids were digested for 3 hours at 37°C at a concentration of 100 ng/μl. Linearization of the *ZIP1* plasmids and vector were expected to make 7.0 kb and 4.2 kb fragments, respectively. Complete digestion of the plasmids was confirmed using an 0.8% agarose gel. Transformants of NH2400 and NH2401 were selected on SD-trp plates for three days at 30°C. To confirm that Trp^+ transformants contained either the *ZIP1* or *zip1-4A* plasmids, colony PCR was performed using ZIP1SEQ12 as the forward primer and ZIP1SEQ19 as the reverse primer to produce a 1 kb fragment. The PCR product was confirmed using an 0.8% agarose gel (data not shown).

The *zip1-4A* mutant exhibits a synthetic meiotic progression defect in heterozygous and homozygous *srs2-md* diploids

To analyze meiotic progression in the *srs2-md* heterozygous and homozygous diploids containing different alleles of *ZIP1*, transformants were first grown overnight in YPD. The overnight cultures were then diluted in YPA medium and shaken at 250 rpm

at 30°C for 16 hours to get the cells into log phase growth. The optical density (OD) from each culture was measured in a spectrophotometer set at a wavelength of 660 nm. To induce meiosis with optimal sporulation conditions, cells with OD_{660} readings of 1.3 – 1.6, (haploid density range 3.22×10^7 – 5.23×10^7) were selected (Lo and Hollingsworth, 2011). The cells were resuspended in Spo medium at a density of 3 X 10^7 cell/mL. 0.5 mL samples were taken at 2 hour intervals over 12 hours, and fixed in 3.7% formaldehyde. The DNA in the cell nuclei was then stained with DAPI and viewed with a fluorescent microscope to examine the number of nuclei present. Mononucleate cells indicate that the cells either did not enter meiosis or were in meiotic prophase, binucleate cells have completed Meiosis I and tetranucleate cells have completed Meiosis II. The percentage of cells completing Meiosis I and Meiosis II were combined to determine the amount of meiotic progression (Figure 6).

The *SRS2/srs2-md ZIP1* diploid progressed through meiosis with rates comparable to NH716 (Callender and Hollingsworth, 2010), which is WT for *SRS2* and *ZIP1*. The first thing to note is that the homozygous *srs2-md ZIP1* strain was delayed two hours relative to the *SRS2/srs2-md ZIP1* diploid, indicating that *srs2-md* alone has a meiotic progression defect. The first signs of Meiosis I were seen at the 4 hour time point, and by the 12 hour time point, 92% of the cells completed MI or MII (Figure 6A). The *zip1*Δ and *zip1-4A* mutants behaved similarly in both the *srs2-md* heterozygous and homozygous diploids. In both backgrounds a more severe phenotype was observed for *zip1-4A* than *zip1*Δ. For example, at the final time point, *SRS2/srs2-md zip1*Δ had 60% more cells that completed MI or MII compared to <10% in the the *SRS2/srs2-md zip1-*

4A strain (Figure 6A). A low amount of bi/tetranucleates was formed by the 12 hour time point for *zip1-4A* in both the *SRS2/srs2-md* and *srs2-md/srs2-md* diploids.

To measure sporulation, colonies of each strain were patched onto YPDcom plates, replica plated to Spo medium and incubated at 30°C for 2 days. Sporulation percentages were averaged from three different experiments for a total of 7 different colonies. The *srs2-md* homozygote sporulated poorly no matter which *ZIP1* allele was present, in contrast to the *SRS2*/*srs2-md* heterozygote. In both heterozygous and homozygous *srs2-md* strains, *ZIP1* had the highest and *zip1-4A* had the lowest percentage of sporulation (Figure 6B). In combination with heterozygous and homozygous *srs2-md* alleles, the presence of *zip1-4A* has a more severe effect on meiosis than not having *ZIP1* at all. This gain of function mutation agrees with the model that was proposed for *SGS1* activity in meiosis. It was proposed that Sgs1 removes Zip1-4A from DSBs, otherwise the break cannot get repaired. Therefore, in the absence of a corrective helicase, it is more conducive for a meiotic central component to be missing instead of defective.

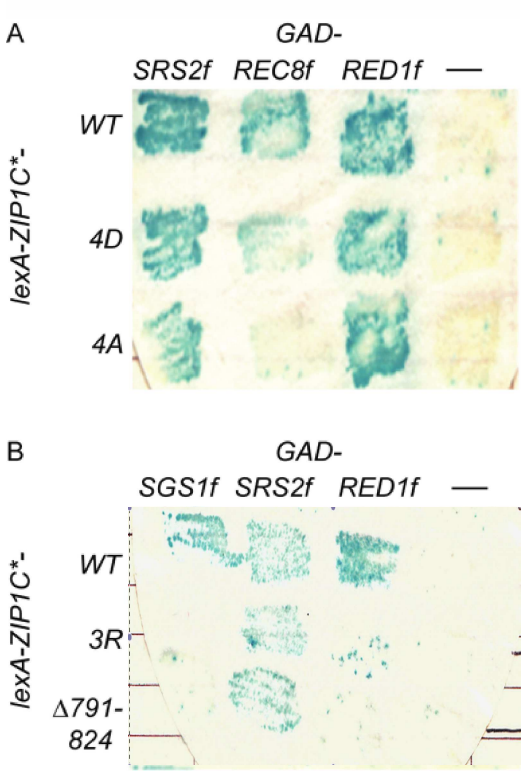

Figure 3. Defining the parameters of the *lexA-ZIP1C*/GAD-SRS4f* interaction using the two-hybrid system. L40 was transformed with plasmids carrying the indicated *lex-ZIP1C** alleles along with various *GAD* fusions. "f" indicates that only a fragment of the gene was fused to *GAD*: codons 81-614 for *SGS1*, 1035-1174 for *SRS2*, 537-827 for *RED1* and 133-433 for *REC8*. The pGAD424 plasmid was used as the *GAD* alone control (-). (A) Two hybrid assays with the *lexA-ZIP1C*-4D* and *4A* alleles and various *GAD*-fusions. The *4A* and *4D* alleles contain S815-818 mutated to alanine or aspartic acid, respectively. (B) Two hybrid assays with the *lexA-ZIP1C*-3R* allele which mutates the SUMO recognition motif by substituting E862, D863 and Q864 for arginine (Lin et al., 2010) (Hussain, 2013)and the *lexA-ZIP1C*-Δ791-824* allele which contains an in-frame deletion of codons 791-824 which are required for synapsis (Tung and Roeder, 1998) (Hussain, 2013)

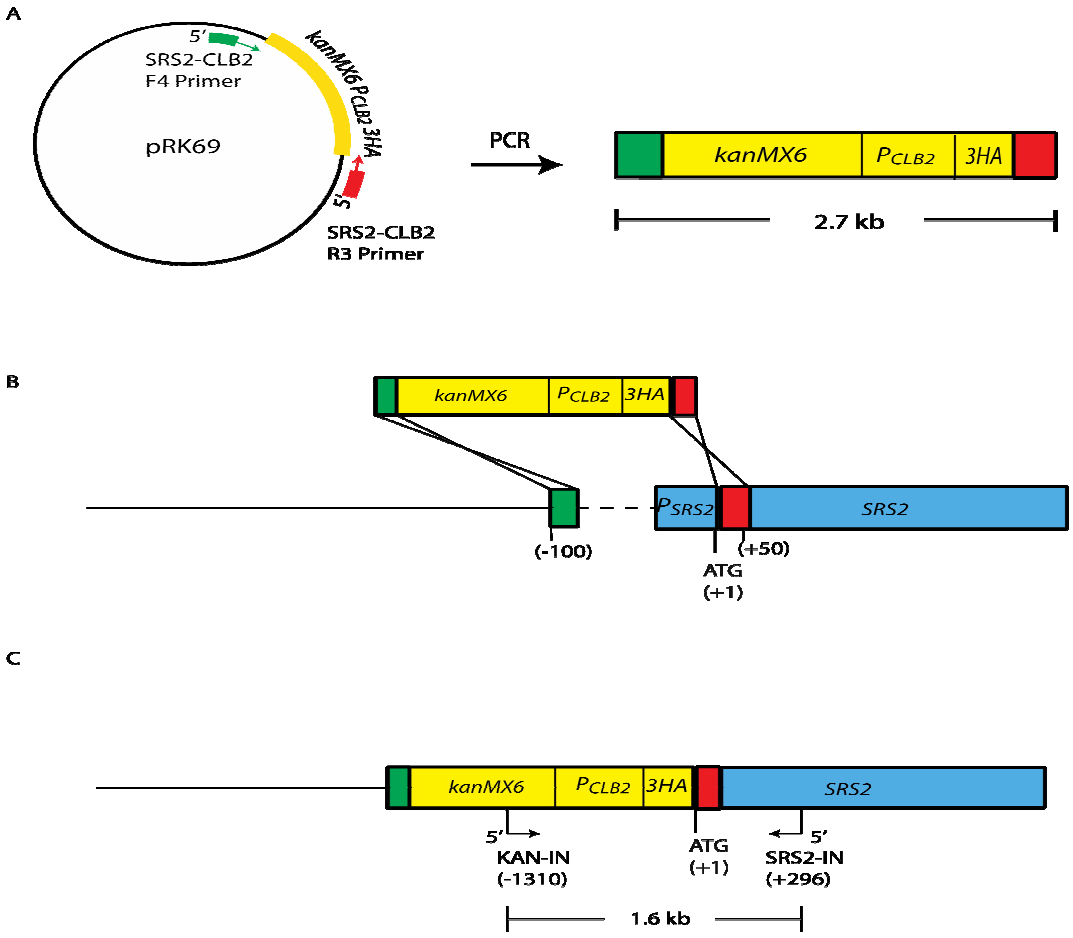

Figure 4. Diagram of the *srs2-md* allele construction. (A) The SRS2-F4 and SRS2-R3 primers were used to amplify a 2.7 kb fragment using pRK69 as the template plasmid. The green box represents 50 bp that start 100 bp 5' to the ATG. The red box represents the 50 bp located immediately 3' of the ATG. Numbers indicate basepairs relative to the ATG. (B) Recombination between the ends of the fragment and the chromosome replaces P_{SRS2} with *kanMX6-*P_{CLB2}*-3HA*. (C) Location of the KAN-IN and SRS2-IN primers used to detect the presence of the PCLB2-3HA-SRS2 (srs2-md) allele.

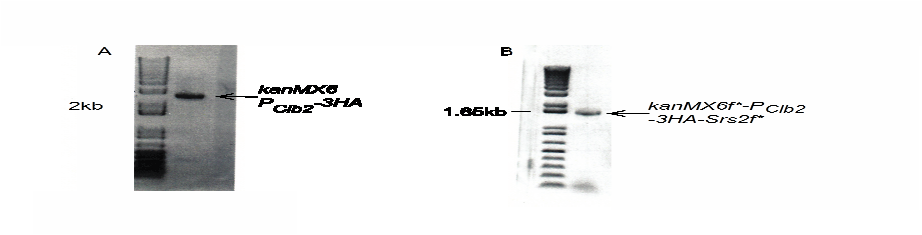

Figure 5. Steps in the construction of *P*$_{CLB2}$*-SRS2* (*srs2-md*). (A) SRS2-CLB2-F4 and SRS2-CLB2-R3 primers were used to amplify a 2.7 kb fragment containing *kanMX6-P*$_{CLB2}$*-3HA.* This fragment is flanked by 50 of DNA located from -100 to -50 bp and 1-50 bp relative to the *SRS2* ATG. (B) SRS2-IN and KAN-IN primers were used for colony PCR to confirm the presence of the *srs2-md* allele. SRS2-IN is a reverse primer that starts 296 bp 3' of the ATG of the fusion site, while KAN-IN is a forward primer located 1.3 kb upstream of the *SRS2* ATG, leading to a predicted fragment size of 1.6 kb. "f*" indicates that only a fragment of the gene was amplified.

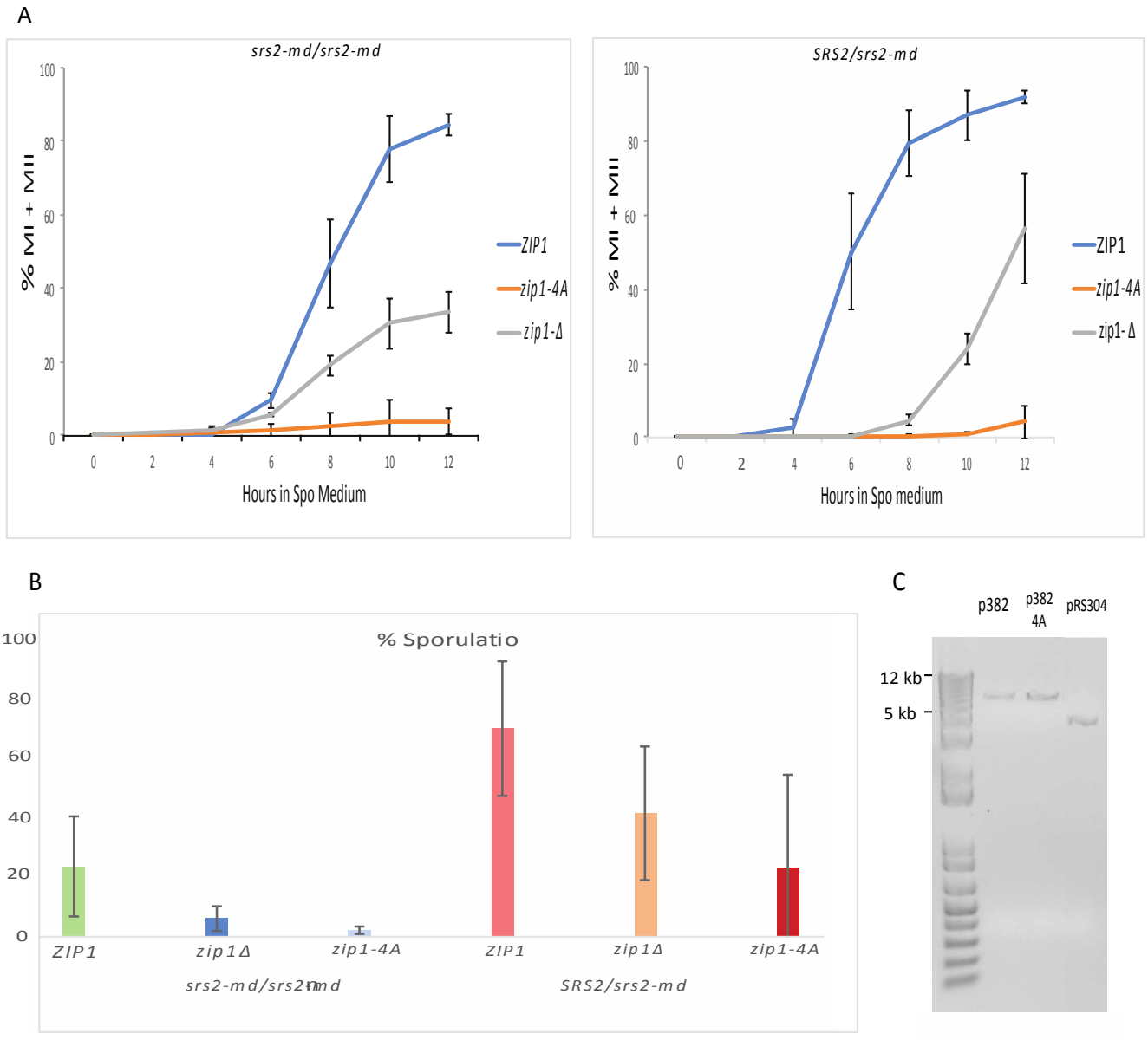

Figure 6. Meiotic and sporulation in diploids containing various combinations of *srs2-md* and *zip1* alleles. (A) DAPI stained cells were quantified in microscope at 40X. In 3 separate meiotic time course experiments , 200 cells were classified as monucleate, binucleate and tetranucleate. Bii and tetranucleate were combined to measure meiotic progression at each time point. (B) Sporulation percentages were generated from seven colonies where 200 cell asci were examined. The error bars show the variability in the repeated experiments (n = 3). (C) p382, p382-4A and pRS304 completely digested with BsgI and ran on a 0.8% agarose gel. p382 and p382-4A linearized fragment size was expected to be 7.2 kb while the pRS304 vector was expected to be 4.2 kb.

Discussion

Interaction of Srs2$^{1035-1174}$ with the Zip1 C-terminus does not require negative charges, sumoylation or the 25 amino acid domain required for synapsis

At the center of the synaptonemal complex, the Zip1 transverse filaments confer synapsis. Zip1 is a multi-functional meiosis-specific protein that juxtaposes homologs and is a site for modifications that promote progression past the recombination checkpoint arrest (Sym et al., 1993; Tung and Roeder, 1998). The Zip1 C terminal domain is essential region synapsis and the ZMM pathway of recombination. Within this region there are 4 serines at residues 815 – 818 (4S). These serines are Cdc7-Dbf4 substrates that regulate the CO/NCO decision and synapsis (Chen et al., 2015). In a *zip1-4A* allele which prevents phosphorylation at these residues, COs and meiotic progression phenotypes were reduced and delayed more than the *zip1Δ* cells. The *zip1-4D* allelle substitutes aspartic acids for the four serines to provide a constitutive negative charge and thus mimic phosphorylation. *zip1-4D* shows WT meiotic phenotypes (Chen et al., 2015). Additionally, the Zip1 C terminus has a SIM which was suggested to mediate an interaction with Srs2's SIM (Murray, 2015). SIMs are known to facilitate or obstruct subsequent protein interactions (Altmannova et al., 2012).

As previously mentioned, Matthew Murray used a yeast two hybrid screen with the *ZIP1* C terminus containing the *4D* mutants to isolate two overlapping fragments of Srs2. The β-galactosidase assays performed for my thesis show that Srs2$^{1035-1174}$ interacts with Zip1-4A, indicating that Srs2's affinity for Zip1 is not mediated by the negative charges at the 4S region. In testing the influence of Zip1's amino acids 791-824 or Zip1's SIM role in recruiting Srs2, β galactosidase assays show that Srs2$^{1035-1174}$

has a reduced affinity for Zip1 but is still able to interact. About 50% of the yeast two hybrid assays did not show an interaction between Srs2$^{1035\text{-}1174}$ with Zip1C*-Δ791-824 or the SIM mutant plasmid. We propose that the range of blue color used to report protein interaction is a consequence of the variability of the 2μ plasmid copy number. The affinity is likely reduced, and in combination with low amounts of plasmid copies can put the prey and bait levels below the threshold needed to activate the reporter. To test this theory, quantitative polymerase chain reactions could be used to quantify the plasmid copy number and determine if the reporter signal corresponds to plasmid copy number (Anindyajati et al., 2016; Tal and Paulsson, 2012).

srs2-md zip1-4A double mutants cause a gain of function phenotype

In both meiotic and vegetative cells Srs2 and Sgs1 helicases are used to reduce the occurrence of detrimental COs, while facilitating repair of DSBs as NCOs to maintain genomic integrity (Ira et al., 2003; Oh et al., 2007).Sgs1 helicase activity has an influence over which recombination pathway will be taken to repair DSBs. In wild-type meiosis Sgs1 dictates early NCO formation via the SDSA pathway, thus in *sgs1-md* cells, NCO formation becomes dependent on the SSN pathway which may equally resolve recombination intermediates into COs (Muyt et al., 2012). Contrary to the SDSA pathway, the *ZMM* genes promotes formation of COs. Particularly, Zip1 phosphorylation promotes resolution of dHJs into COs that exhibit interference (Chen et al., 2015). There is an antagonistic relationship between Sgs1 and Zip1, where before phosphorylation takes place, Sgs1 may act on uncommitted recombination intermediates to unwind Rad51 filaments and allow strand invasion to restart to correct

the aberrant intermediates, or be routed to the SDSA pathway. Chen et al. used an *sgs1-md* allele to identify that the absence of *sgs1* caused a slight reduction in sporulation, with near WT rates of meiotic progression, and increased CO levels. When *sgs1-md* was combined with *zip1-4A*, sporulation was significantly reduced to ~10% and at the 12 hour time point meiotic progression was ~5%. The surprising result gained from this study was that *sgs1-md zip1-Δ* had better meiotic progression and sporulation than *sgs1-md zip1-4A*. The *sgs1-md zip1-4A* gain of function phenotype suggests that it is worse to have unphosphorylated Zip1 protein than to not have *ZIP1* at all. Chen et al proposed that *sgs1-md* is unable to dissociate zip1-4A from DSBs. Therefore the break cannot be repaired. Consequently, this results in meiotic prophase arrest (Lydall et al., 1996). The *sgs1-md zip1Δ* can progress because eventually it is able to downregulate Spo11 activity (Chen et al., 2015).

Homozygous *srs2-md* showed similar delays in meiotic progression to the *sgs1-md* experiments. To test our explanation that the meiotic progression delay is a consequence of unrepaired DSBs, a *spo11* mutant that does not make any DSBs could be introduced into the *srs2-md/srs2-md zip1-4A* (Keeney, 2008). The lack of DSBs is expected to rescue the delay. It would be interesting to see if *spo11*Δ also rescues the delay in the *srs2-md* homozygote compared to the heterozygote, which would suggest a role for *SRS2* in meiotic recombination. When the meiotic depletion alleles were combined with *zip1* mutants, meiotic progression and sporulation was further reduced and the *zip1-4A* gain of function phenotype was expressed. A surprising result appeared in the *srs2-md* diploid strain where there was a drastic reduction in sporulation although the cells progressed through meiosis appropriately. A possible

explanation for this phenotype is the lack of Srs2 activity allows for enough DSBs to be repaired to progress past the checkpoints, but the deficiency in Srs2 confers increased CO levels that may be sub-optimal and thus defects the ability to form asci.

The fact that heterozygous *SRS2/srs2-md zip1-4A* failed to progress suggests that one copy of *SRS2* is not enough to dissociate the defective *zip1-4A*. To test this idea, an additional *SRS2* allele should be transformed into heterozygous *SRS2/srs2-md*. If the additional WT allele can rescue meiotic progression, this would support the idea that *SRS2* is haploid insufficient for meiotic progression in the *zip1-4A* background.

The results gained from Chen et al. in combination with the data in this thesis lead to the question of whether there is redundancy between *SGS1* and *SRS2* for meiotic recombination. They are both 3' to 5' helicases used to regulate CO/NCO resolution, yet the absence of either one of the helicases in combination with the z*ip1-4A* reduces sporulation percentages drastically. If the two helicases functioned redundantly, a single helicase mutant with *zip1-4A* should not have a phenotype, because the second helicase would compensate for the mutant helicase. The fact that both *srs2-md zip1-4A* and *sgs1-md zip1-4A* demonstrated such severe phenotypes suggest that these are not redundant genes. An alternative possibility is that Srs2 and Sgs1 function together, perhaps as a protein complex. Co-immunoprecipitation experiments could be used to test this idea.

.

Table 1. Yeast Strains

Strain[a]	Genotype	Source
L40	*MAT***a** *his3Δ200 trp1-90 leu2-2,112 ade2 lys2::lexA$_{op}$-HIS3::LYS2 ura3::lexA$_{op}$-lacZ::URA3*	(Woltering et al., 2000)
NHY1215 trp1 zip1::NAT XC	*MATα leu2::hisG his4-X::LEU2-(NGOMIV + ori) trp1-5'Δ::hphMX4 zip1Δ::natMX4*	Hollingsworth
NHY1215 trp1 zip1::NAT XC srs2-md	*MATα leu2::hisG his4-X::LEU2-(NGOMIV + ori) trp1-5'Δ::hphMX4 zip1Δ::natMX4 kanMX6::P$_{CLB2}$-3HA-SRS2*	Dimitri Joseph
NHY1210 trp1	*MAT***a** *leu2::hisG HIS4::LEU2-(Bam+ ori) ho::hisG ura3(ΔSma-Pst) trp1-5'Δ::hphMX4*	Hollingsworth
NHY2393 6-4	*MAT***a** *leu2::hisG HIS4::LEU2-(Bam+ ori)) ho::hisG ura3(ΔSma-Pst) trp1-5'Δ::hphMX4 zip1Δ::natMX4 kanMX6::P$_{CLB2}$-3HA-SRS2*	Dimitri Joseph
NH2400	*MAT***a** *leu2::hisG HIS4::LEU2-(Bam+ ori)) ho::hisG ura3(ΔSma-Pst) trp1-5'Δ :: hphMX4* *MATα leu2::hisG his4-X::LEU2-(NGOMIV + ori) trp1-5'Δ::hphMX4 zip1Δ::natMX4 SRS2 zip1Δ::natMX4 kanMX6::P$_{CLB2}$-3HA-SRS2*	Dimitri Joseph

NH2401	*MAT**a** leu2::hisG HIS4::LEU2-(Bam+ ori)) ho::hisG ura3(ΔSma-Pst) trp1-5'Δ::hphMX4 MATα leu2::hisG his4-X::LEU2-(NGOMIV + ori) trp1-5'Δ::hphMX4 zip1Δ::natMX4 kanMX6::P_{CLB2}-3HA-SRS2 zip1Δ::natMX4 kanMX6::P_{CLB2}-3HA-SRS2*	Dimitri Joseph
NH716	*MATα leu2::hisG his4-X::LEU2(NgoMIV+ ori) hoΔ::hisG ura3(Δpst-sma)* *MAT**a** leu2::hisG HIS4::LEU2(BamH + oriI) hoΔ::hisG ura3(Δpst-sma)*	Neil Hunter

Table 2. Primer sequences

Primer	Sequence
SRS2-CLB2-F4	5’ TTCCTGTCCCTCTAGTTTCTTTTGCCATCCATAATTGTA CTCTGCACTTTGAATTCGAGCTCGTTTAAAC 3’
SRS2-CLB2-R3	5’ AGTATTTAACTGGGATACTAAATGCAACCAAAGATCA TTGTTCGACGACATGCACTGAGCAGCGTAATCTG 3’
KAN-IN	5’ GCCGTAATTTTTGCTTCGCGC 3’
SRS2-IN	5’ AAAAGTACCAATTAAGAG 3’
ZIP1-SEQ12	5’ GGTGAAGGCATATAAGGC 3’
ZIP1-SEQ19	5’ TGGTTTAATTTGGATTGG 3’

Table 3. Plasmids

Plasmid name	Relevant yeast genotype	Source
pBTM116-ZIP1C* WT	2µ *amp^R TRP1 lexA-ZIP1C*-WT*	(Chen et al., 2015)
pBTM116-ZIP1C*-4A	2µ *amp^R TRP1 lexA-ZIP1C*-S815A S816A S817A S818A*	(Chen et al., 2015)
pBTM116-ZIP1C*-4D	2µ *amp^R TRP1 lexA-ZIP1C*-S815D S816D S817D S818D*	(Chen et al., 2015)
pGAD424	2µ *amp^R LEU2, GAD*	(Chien et al., 1991)
pGAD-RED1$^{537-827}$	2µ *amp^R LEU2 GAD-RED1$^{537-827}$*	(Tu et al., 1996)
pGAD-REC8	2µ *amp^R LEU2 GAD-REC8*	(Murray, 2015)
pGAD-SGS1$^{81-614}$	2µ *amp^R GAD-SGS1$^{81-614}$*	(Hussain, 2013)
pGAD-SRS2$^{1035-1174}$	2µ *amp^R GAD-SRS$^{1035-1174}$*	(Murray, 2015)
pSH1	2µ *amp^R TRP1 lexA-ZIP1C*-3R*	(Hussain, 2013)
pSH2	2µ *amp^R TRP1 lexA- ZIP1-C*-Δ791-824*	(Hussain, 2013)
pRK69	*amp^R P_{CLB2}-3HA kanMX6*	Michael Lichten
pRS304	*amp^R TRP1*	Robert Sikorski
p382	*ZIP1 TRP1 amp*	Andreas Hochwagen
p382-4A	*ZIP1-S815A S816A S817A S818A TRP1 amp*	(Chen et al., 2015)

Table 3. Primer sequences

Primer	Sequence
SRS2-CLB2-F4	5’ TTCCTGTCCCTCTAGTTTCTTTTGCCATCCATAATTGTA CTCTGCACTTTGAATTCGAGCTCGTTTAAAC 3’
SRS2-CLB2-R3	5’ AGTATTTAACTGGGATACTAAATGCAACCAAAGATCA TTGTTCGACGACATGCACTGAGCAGCGTAATCTG 3’
KAN-IN	5’ GCCGTAATTTTTGCTTCGCGC 3’
SRS2-IN	5’ AAAAGTACCAATTAAGAG 3’
ZIP1-SEQ12	5’ GGTGAAGGCATATAAGGC 3’
ZIP1-SEQ19	5’ TGGTTTAATTTGGATTGG 3’

References

Allers, T., and Lichten, M. (2001). Differential Timing and Control of Noncrossover and Crossover Recombination during Meiosis. Cell *106*, 47-57.

Altmannova, V., Kolesar, P., and Krejci, L. (2012). SUMO wrestles with Recombination. Biomolecules *2*, *350-375*.

Anindyajati, Artarinin, A.A., Riani, C., and Retnoningrum, D.S. (2016). Plasmid Copy Number Determination by Quantitaive Polymerase Chain Reaction. Scientia Pharmaceutica *84*, 89-101.

Antony, E., Tomko, E.J., Xiao, Q., Krejci, L., Lohman, T.M., and Ellenberger, T. (2009). Srs2 disassembles Rad51 filaments by a protein-protein interaction triggering ATP turnover and dissociation of Rad51 from DNA. Mol Cell *35*, 105-115.

Borner, G.V., Kleckner, N., and Hunter, N. (2004). Crossover/Noncrossover Differentiation, Synaptonemal Complex formation, and Regulatory Surveillance at the Leptotene/Zygotene Transition of Meiosis. Cell *117*, 29-45.

Brown, M.S., Grubb, J., Zhang, A., Rust, M.J., and Bishop, D.K. (2015). Small Rad51 and Dmc1 Complexes Often Co-occupy Both Ends of a Meiotic DNA Double Strand Break. PLoS Genet *11*, e1005653.

Callender, T.L., and Hollingsworth, N.M. (2010). Mek1 suppression of meiotic double-strand break repair is specific to sister chromatids, chromosome autonomous and independent of Rec8 cohesin complexes. Genetics *185*, 771-782.

Chen, X., Suhandynata, R.T., Sandhu, R., Rockmill, B., Mohibullah, N., Niu, H., Liang, J., Lo, H.C., Miller, D.E., Zhou, H.*, et al.* (2015). Phosphorylation of the Synaptonemal Complex Protein Zip1 Regulates the Crossover/Noncrossover Decision during Yeast Meiosis. PLoS Biol *13*, e1002329.

Cheng, C.H., Lo, Y.H., Liang, S.S., Ti, S.C., Lin, F.M., Yeh, C.H., Huang, H.Y., and Wang, T.F. (2006). SUMO modifications control assembly of synaptonemal complex and polycomplex in meiosis of Saccharomyces cerevisiae. Genes Dev *20*, 2067-2081.

Chien, C.-T., Bartel, P.L., Sternglanz, R., and Fields, S. (1991). The two-hybrid System: A method to identify and clone genes for proteins that interact with a protein of interest. Proc Natl Acad Sci *88*, *9578-9582*.

Clark-Walker, G.D., and Miklos, G.L.G. (1974). Localization and Quantification of Circular DNA in Yeast. The FEBS Journal *41*, *359-365*.

Criekinge, W.V., and Beyaert, R. (1999). Yeast Two-Hbrid:State of the Art. Biological Procedures Online *2*, *1-38*.

Dahmann, C., and Futcher, B. (1995). Specialization of B-Type Cyclins for Mitosis or Meiosis in *S.cerevisiae*, *C.S.H. Laboratory*, ed. (Cold Spring Harbor, New York, 11724).

Dunn, C.D., Lee, M.S., Spencer, F.A., and Jensen, R.E. (2005). A Genomewide Screen for PEtite-negative Yeast Strains Yields a New Subunit of the i-AAA protease Complex. Molecular biology of the Cell *17*, 213-226.

Esta, A., Ma, E., Dupaigne, P., Maloisel, L., Guerois, R., Le Cam, E., Veaute, X., and Coic, E. (2013). Rad52 sumoylation prevents the toxicity of unproductive Rad51 filaments independently of the anti-recombinase Srs2. PLoS Genet *9*, e1003833.

Goldstein, A.L., and McCusker, J.H. (1999). Three New Dominant Drug Resistance Cassettes for GeneDisruptin in *Saccharomyces cerevisae*. Yeast *15*, *1541-1553*.

Hentges, P., Van Driessche, B., Tafforeau, L., Vandenhaute, J., and Carr, A.M. (2005). Three novel antibiotic marker cassettes for gene disruption and marker switching in Schizosaccharomyces pombe. Yeast *22*, 1013-1019.

Hussain, S. (2013). Analysis of Zip1 and Sgs1 protein interaction in budding yeast. In Biochemistry and Cell Biology (Stony Brook University).

Ira, G., Malkova, A., Liberi, G., Foiani, M., and Haber, J.E. (2003). Srs2 and Sgs1-Top3 Suppress Crossovers during Double-Strand Break Repair in Yeast. Cell *115*, 401-411.

Jessop, L., and Lichten, M. (2008). Mus81/Mms4 Endonuclease and Sgs1 Helicase Collaborate to Ensure Proper Recombination Intermediate Metabolism during Meiosis. Molecular Cell *31*, 313-323.

Jessop, L., Rockmill, B., Roeder, G.S., and Lichten, M. (2006). Meiotic chromosome synapsis-promoting proteins antagonize the anti-crossover activity of sgs1. PLoS Genet *2*, e155.

Karen Voelkel-Meiman, Louis F. Taylor, Pritam Mukherjee, Neil Humphryes, Hideo Tsubouchi, and MacQueen, A.J. (2013). SUMO Localizes to the Central Element of

Synaptonemal Complex and Is Required for the Full Synapsis of Meiotic Chromosomes in Budding Yeast. Plos Genetics *9*, e1003837.

Keeney, S. (2008). Spo11 and the Formation of DNA Double-Strand Breaks in Meiosis. Genome Dyn Stab *2*, 81-123.

Keeney, S., Giroux, C.N., and Kleckner, N. (1997). Meiosis-Specific DNA Double-Strand Breaks Are Catalyzed by Spo11, a Member of a Widely Conserved Protein Family. Cell *88*, 375-384.

Klein, F., MAhr, P., Galove, M., Buonomo, S.B.C., Michaelis, C., Nairz, K., and Nasmyth, K. (1999). A Central Role for Cohesins in sister Chromatid Cohesion, Formation of Axial elements and Recombination during Yeast Meiosis. cell *98*, 91-103.

Krejci, L., Komen, S.V., Li, Y., Villemain, J., Reddy, M.S., Klein, H., Ellenberger, T., and Sung, P. (2003). DNA helicase Srs2 disrupts the Rad51 presynaptic filament. Nature *423*, 305-309.

Lin, F.M., Lai, Y.J., Shen, H.J., Cheng, Y.H., and Wang, T.F. (2010). Yeast axial-element protein, Red1, binds SUMO chains to promote meiotic interhomologue recombination and chromosome synapsis. EMBO J *29*, 586-596.

Lo, H.C., and Hollingsworth, N.M. (2011). Using the semi-synthetic epitope system to identify direct substrates of the meiosis-specific budding yeast kinase, Mek1. Methods Mol Biol *745*, 135-149.

Lydall, D., Nikolsky, Y., Bishop, D., and Weinert, T. (1996). A meiotic recombination checkpoint controlled by mitotic checkpoint genes. Nature *383*, 840-843.

Lynn, A., Soucek, R., and Borner, G.V. (2007). ZMM proteins during meiosis: crossover artists at work. Chromosome Res *15*, 591-605.

McMahill, M.S., Sham, C.W., and Bishop, D.K. (2007). Synthesis-dependent strand annealing in meiosis. PLoS Biol *5*, e299.

Murray, M. (2015). Identification of binding partners with the negatively charged Zip1 C-terminus using a two-hybrid screen. In Biochemistry and Cell Biology (Stony Brook University).

Muyt, A.D., Jesso, L., Kolar, E., Sourirajan, A., Chen, J., Dayani, Y., and Lichten, M. (2012). BLM helicase ortholog Sgs1 is a central regulator of meotic recombination intermediate metabolism. Molecular Cell *46*, 43-53.

Niu, H., wan, L., Baumgartner, B., Schaefer, D., Loidl, J., and Hollingsworth, N.M. (2005). Partner Choice during Meiosi Is Regulated by Hop1-promoted Dimerization of Mek1. Molecular biology of the Cell *16*, 5804-5818.

Oh, S.D., Lao, J.P., Hwang, P.Y., Taylor, A.F., Smith, G.R., and Hunter, N. (2007). BLM ortholog, Sgs1, prevents aberrant crossing-over by suppressing formation of multichromatid joint molecules. Cell *130*, 259-272.

Page, S.L., and Hawley, R.S. (2004). The genetics and molecular biology of the synaptonemal complex. Annu Rev Cell Dev Biol *20*, 525-558.

Roeder, G.S., and Bailis, J.M. (2000). The pachytene checkpoint. Trends in Genetics *16*, 395-403.

Sasanuma, H., Furihata, Y., Shinohara, M., and Shinohara, A. (2013). Remodeling of the Rad51 DNA Strand -Exchange Protein by the Srs2 Helicase. Genetics *194*, 859-872.

Shinohara, A., Gasior, S., Ogawa, T., Kleckner, N., and Bishop, D.K. (1997). *Saccharomyces cerevisiae recA* homologues *RAD51* and *DMC1* have both distinct and overlapping roles in meiotic recombination. Genes to Cells *2*, 615-629.

Shinohara, M., Hayashihara, K., Grubb, J.T., Bishop, D.K., and Shinohara, A. (2015). DNA damage response clamp 9-1-1 promotes assembly of ZMM proteins for formation of crossovers and synaptonemal complex. Journal of Cell Science *128*.

Smith, A.V., and Roeder, G.S. (1997). The Yeast Red1 Protein Localized to the Cores of Meiotic Chromosomes. Journal of Cell Biology *136*, 957-967.

Sternglanz, S.F.a.R. (1994). The two-hybrid system: an assay for protein-protein interactions. Trends in Genetics *10*, 286-292.

Sym, M., Engebrecht, J., and Roeder, G.S. (1993). Zip1 is a synaptonemal complex protein required for meiotic chromosome synapsis. Cell *72*, 365-378.

Tal, S., and Paulsson, J. (2012). Evaluating quantitaive methods for measuring plasmid copy numbers in single cells. In Plasmid, H.A. Manuscript, ed., pp. 167-173.

Thacker, D., Mohibullah, N., Zhu, X., and Keeney, S. (2014). Homologue engagement controls meiotic DNA break number and distribution. Nature *510*, 241-246.

Tu, J., Song, W., and Carlson, M. (1996). Protein Phospatase Type I Interacts with Proteins Required for Meiosis and Other Cellular Processes in Saccharomyces cerevisiae. Molecular and Cell Biology *16*, 4199-4206.

Tung, K., and Roeder, G.S. (1998). Meiotic Chromosome Morphology and Behavio in zip1 Mutants of Saccaromyces cervisiae. Genetics *149*, 817-832.

Wang, Y., and Dasso, M. (2009). SUMOylation and deSUMOylation at a glance. J Cell Sci *122*, 4249-4252.

Watt, P.M., Hickson, I.D., Borts, R.H., and Louis, E.J. (1996). Sgs1, a Homologue of the Bloom's and Werner's Genes, Is required for Maintenance of Genome Stability in Saccharomyces Cerevisiae. Genetics *144*, 935-945.

Woltering, D., Baumgartner, B., Bahcgi, S., Larkin, B., Loidl, J., Santos, T.d.L., and Hollingsworth, N.M. (2000). Meiotic Segrgation, Synapsis and Recombination Checkpoint Functions Require Physical Interaction between the Chromosmal Proteins Red1p and Hop1p. Molecular and Cell Biology *20*, 6646-6658.